A new semi-analytic approach for class-E resonant DC-DC converter design

This is the author's version of the article that has been presented at IEEE ISCAS2015
The editorial version of the paper is available at http://dx.doi.org/10.1109/ISCAS.2015.7169189

A New Semi-Analytic Approach for Class-E Resonant DC-DC Converter Design

Nicola Bertoni*, Giovanni Frattini§, Roberto Massolini§, Fabio Pareschi*,‡, Riccardo Rovatti†,‡, Gianluca Setti*,‡
* ENDIF – University of Ferrara, via Saragat 1, 44122 Ferrara, Italy. email:{nicola.bertoni, fabio.pareschi, gianluca.setti}@unife.it
† DEI – University of Bologna, viale del Risorgimento 2, 40136 Bologna, Italy. email:riccardo.rovatti@unibo.it
‡ ARCES – University of Bologna, via Toffano 2, 40125 Bologna, Italy
§Texas Instruments Italia, 20089 Rozzano, Italy email:{giovanni.frattini, roberto.massolini}@ti.com

***Abstract*—This paper presents a new approach for the design of a class-E resonant dc-dc converter. The small number of passive components featured by the considered topology allows to exactly solve the differential equations regulating the circuit evolution, and to develop a semi-analytic design procedure based on the differential equations solution. This represents an important breakthrough with respect to the state-of-the-art, where class-E circuit analysis is always based on strong simplifying assumptions, and the exact circuit design is achieved by means of numerical simulations after many time-consuming parametric sweeps.**

I. Introduction

The need for high-efficiency dc-dc power converters operating at increasing switching frequencies (up to the VHF range, 30–300 MHz), with better transient performance and bandwidth, and allowing the use of fully integrated air-core magnetics (with remarkable benefits in terms of both size and cost), leads to the design of new architectures aiming at the minimization of the switching losses [1].

In this paper we focus on class-E resonant power converters [2], [3], [4], [5]. These circuits exploit the so called *soft-switching* technique in order to reduce the switching losses. Conversely from classic (class-D) switching converters, characterized by rectangular waveforms, class-E converters embed a resonant circuit that, roughly speaking, shapes the drain-to-source voltage V_{DS} and the drain current I_{DS} of the MOS switch with a sinusoidal-like form, synchronizing the zero-crossing instants of V_{DS} and I_{DS} with the turn-on instant of the MOS switch. These approaches are known, respectively, as zero-voltage switching (ZVS) and zero-current switching (ZCS), and they are used to reduce the voltage-current product of the MOS at the switching instants, thus lowering (ideally, down to zero) the energy-loss-per-cycle, reducing the device stress and relaxing the constraints on the switch turn-on and turn-off response times. In other words, these approaches allow the desired increase in the switching frequency.

However, the design of a class-E converter is not a trivial task. In fact, the state-of-the-art methodology is based on the simplifying assumption that the circuit can be conveniently separated into a class-E inverter [6], followed by a class-E rectifier [7]. Then, assuming to address the connection between the inverter and rectifier sections by means of a high-Q low-pass LC network, the rectifier can be designed by considering the inverter as a sinusoidal voltage source and the inverter is designed by replacing the rectifier with its equivalent input impedance. In this way one can split the whole converter design into two simplified procedures, but at the cost of accuracy. To achieve the desired behavior, the obtained design is usually refined by means of additional time-consuming transient simulations and extensive sweeps across circuit parameters.

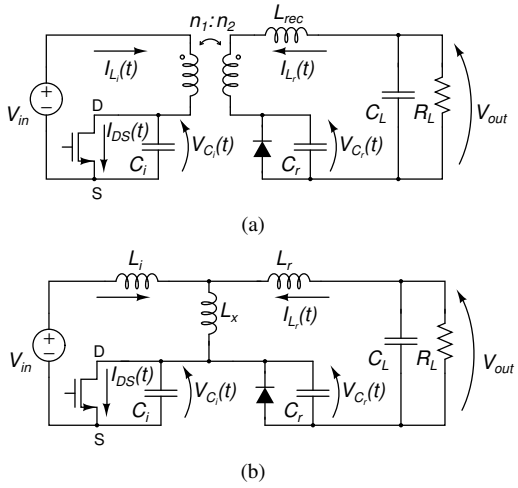

Fig. 1. (a) Schematic of the proposed isolated class-E resonant dc-dc converter; (b) Equivalent circuit of the converter referred to the primary side.

The purpose of this work is to present a new semi-analytic design methodology for the particular class-E dc-dc power converter topology of Fig. 1. Given the low part-count of the considered architecture, the differential equations regulating the circuit behavior can be studied and analytically solved for all possible circuit configurations, *i.e.*, all possible sequences of states in which active devices (transistor and diode) can be found. Then, the converter evolution can be appropriately written as a piece-wise combination of the achieved solutions. Finally, given the exact analytic expression for the converter evolution, it is possible to numerically find the parameters values (in particular of circuit passive elements) ensuring both the requested ZVS/ZCS operating conditions and the desired specifications such as output voltage, switching frequency, *etc.*, without the need of any additional parameter trimming.

The paper is organized as follows. Section II includes the description of the considered converter topology. Section III delineates how to compute the exact analytic expression of the circuit evolution, while in Section IV we exploit this expression for circuit design purposes with an example of a 30 MHz resonant converter. Finally, we draw the conclusion.

II. Class-E Converter Topology

The circuit we consider in this paper is the class-E resonant converter depicted in Fig. 1, either in its isolated or non-isolated configuration as, respectively, in Fig. 1(a) and 1(b). For the sake of simplicity, but without loss of generality, we focus

This is the author's version of the article that has been presented at IEEE ISCAS2015
The editorial version of the paper is available at http://dx.doi.org/10.1109/ISCAS.2015.7169189

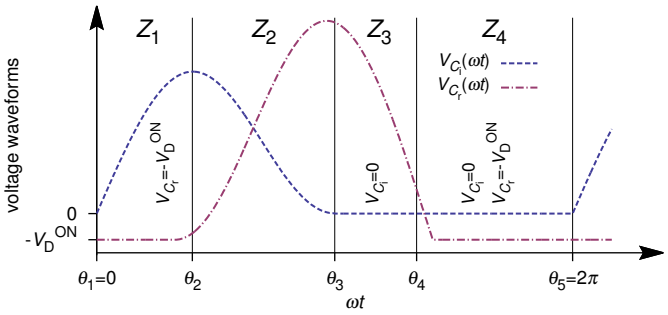

Fig. 2. Class-E converter voltage waveforms with angular time line division based on switching devices ON/OFF state.

on the circuit of Fig. 1(b), keeping in mind that this circuit topology is perfectly equivalent to the isolated one when the transformer is replaced by an equivalent "T" inductor network and when all the elements connected to the secondary side are replaced with the equivalent ones referred to the primary side. Here the inductance L_i represents the leakage part of transformer primary inductance, that can be expressed as $L_\mathrm{i} = \frac{1-k}{k} L_\mathrm{x}$ where k is the well known *coupling coefficient*, and L_r is the equivalent of two actual inductances, the secondary windings leakage one and the rectifying inductance L_rec of Fig. 1(a).

The key feature of this topology is the minimal reactive components (*i.e.*, capacitors and inductors) count. In fact, the main differences between the converter of Fig. 1 and conventional ones is the absence of the usually employed RF choke inductor at the converter input [3] and of any kind of additional filtering/matching network between inverter and rectifier [1], [3], [5]. This has a twofold advantage. First, it makes this solution very appealing for high power density circuits or when the aim is circuit integration. Furthermore, it allows us, as detailed in the following sections, to develop an exact and semi-analytic procedure to achieve the proper design of reactive elements that ensure low-loss (*i.e.*, ZVS and ZCS) operation.

Note that the purpose of this work is limited to define a procedure for the converter power section design. The employment of either a self-resonant gate driver network to reduce the so-called *gating loss*, or a proper feedback control circuitry to cope, for example, with a variable load R_L, will not be discussed.

III. Differential Equation Analysis

In this section, we provide a piecewise analytical description of the circuit behavior based on the exact solution of differential equations. This approach, despite commonly adopted in other application fields, has never been applied to resonant converters, being always considered a cumbersome and unfruitful task [8].

The first assumption we make is that all components are ideal, *i.e.*, that active semiconductor devices are ideal switches with zero ON-resistance and infinite OFF-resistance and reactive elements have an indefinitely high Q factor. As additional hypothesis, we assume that the capacitor C_L is large enough to keep the voltage V_{out} constant, thus allowing to replace the $R_L - C_L$ network with an ideal dc voltage source. The only non-ideality we consider is that the diode has a forward voltage drop equal to $V_D{}^{\mathrm{ON}}$.

By modeling the active devices as ideal switches, one can distinguish four different configurations for the overall circuit, depending on the MOS and diode ON/OFF state. These configurations, referred to as *zones*, are actually four different linear systems that can be studied with the four state variables given by the voltage signals V_{C_i} and V_{C_r} across C_i and C_r and the currents I_{L_i} and I_{L_r} flowing through L_i and L_r. These signals are also highlighted in Fig. 1(b). The differential equations for all configurations can be achieved by considering the Kirchhoff Voltage Laws (KVLs) around both inverter and rectifier closed loops as follows:

$$\begin{cases} \omega\left(L_\mathrm{i}+L_\mathrm{x}\right)\dfrac{dI_{L_\mathrm{i}}(\omega t)}{d\omega t} + \omega L_\mathrm{x}\dfrac{dI_{L_\mathrm{r}}(\omega t)}{d\omega t} + V_{C_\mathrm{i}}(\omega t) - V_{in} = 0 \\ \omega L_\mathrm{x}\dfrac{dI_{L_\mathrm{i}}(\omega t)}{d\omega t} + \omega\left(L_\mathrm{r}+L_\mathrm{x}\right)\dfrac{dI_{L_\mathrm{r}}(\omega t)}{d\omega t} + V_{C_\mathrm{r}}(\omega t) - V_{out} = 0 \end{cases} \tag{1}$$

where $\omega t = 2\pi f_s\, t$ (f_s is the switching frequency). Furthermore, while the MOS switch is ON, the node connecting the drain terminal with the capacitor C_i is shorted to ground

$$V_{C_\mathrm{i}}(\omega t) = 0 \tag{2}$$

while, during the MOS OFF-state period, we have

$$I_{L_\mathrm{i}}(\omega t) = \omega C_\mathrm{i}\frac{dV_{C_\mathrm{i}}(\omega t)}{d\omega t} \tag{3}$$

When the rectifying diode is ON, the voltage V_{C_r} is fixed by the diode forward drop

$$V_{C_\mathrm{r}}(\omega t) = -V_D{}^{\mathrm{ON}} \tag{4}$$

while, when the diode is OFF, the following relation holds

$$I_{L_\mathrm{r}}(\omega t) = \omega C_\mathrm{r}\frac{dV_{C_\mathrm{r}}(\omega t)}{d\omega t} \tag{5}$$

The evolution of each zone is regulated by a different set of equations taken among (1), (2), (3), (4) and (5).

Then, the behavior of the overall converter can be achieved by combining the evolution of the four zone in the order in which, once the steady state is achieved, every zone follows each other. Despite the fact that this order is not known *a priori* since the diode is a non-controlled switch, we limit ourselves to consider the most commonly observed one that corresponds to the sequence depicted in Fig. 2. The horizontal axis, representing the angular time ωt, is divided into the four zones

$$Z_j = \{\,\omega t \,|\, \theta_j \le \omega t < \theta_{j+1}\} \quad j = 1,2,3,4$$

with $\theta_1 = 0$ and $\theta_5 = 2\pi$, while the vertical axis shows the typical V_{C_i} and V_{C_r} waveforms.

Then, referring to the state variables in each zone with the notation below

$$\begin{cases} I_{L_\mathrm{i}}^{(j)}(\omega t) = I_{L_\mathrm{i}}(\omega t) & : \omega t \in Z_j \\ I_{L_\mathrm{r}}^{(j)}(\omega t) = I_{L_\mathrm{r}}(\omega t) & : \omega t \in Z_j \\ V_{C_\mathrm{i}}^{(j)}(\omega t) = V_{C_\mathrm{i}}(\omega t) & : \omega t \in Z_j \\ V_{C_\mathrm{r}}^{(j)}(\omega t) = V_{C_\mathrm{r}}(\omega t) & : \omega t \in Z_j \end{cases}$$

the converter evolution is obtained as follows.

This is the author's version of the article that has been presented at IEEE ISCAS2015
The editorial version of the paper is available at http://dx.doi.org/10.1109/ISCAS.2015.7169189

For $\omega t \in Z_1$ equations (1), (3) and (4) hold, giving rise to the third order system

$$\begin{cases} \omega^2 C_{\rm i}\left(L_{\rm i}+L_{\rm x}\right)\dfrac{d^2 {V_{C_{\rm i}}}^{(1)}(\omega t)}{d(\omega t)^2}+\omega L_{\rm x}\dfrac{d{I_{L_{\rm r}}}^{(1)}(\omega t)}{d\omega t}+{V_{C_{\rm i}}}^{(1)}(\omega t)-V_{in}=0 \\ \omega^2 C_{\rm i}L_{\rm x}\dfrac{d^2 {V_{C_{\rm i}}}^{(1)}(\omega t)}{d(\omega t)^2}+\omega(L_{\rm r}+L_{\rm x})\dfrac{d{I_{L_{\rm r}}}^{(1)}(\omega t)}{d\omega t}-{V_D}^{\rm ON}-V_{out}=0 \end{cases} \tag{6}$$

subject to the initial conditions

$$\begin{cases} {V_{C_{\rm i}}}^{(1)}(0)=0 \\ \left.\dfrac{d{V_{C_{\rm i}}}^{(1)}(\omega t)}{d\omega t}\right|_{\omega t=0}=\dfrac{{I_{L_{\rm i}}}^{(1)}(0)}{\omega C_{\rm i}}=\dfrac{I_{L_{\rm i}}^0}{\omega C_{\rm i}} \\ {I_{L_{\rm r}}}^{(1)}(0)=I_{L_{\rm r}}^0 \end{cases} \tag{7}$$

where $I_{L_{\rm i}}^0$ and $I_{L_{\rm r}}^0$ are unknowns to be determined. The equations (6) can be easily decoupled by substitution into the following second and first order differential equations:

$$\omega^2 C_{\rm i}\left(L_{\rm i}+L_{\rm x}-\frac{{L_{\rm x}}^2}{L_{\rm r}+L_{\rm x}}\right)\frac{d^2 {V_{C_{\rm i}}}^{(1)}(\omega t)}{d(\omega t)^2}+{V_{C_{\rm i}}}^{(1)}(\omega t)-V_{in}+\frac{L_{\rm x}}{L_{\rm r}+L_{\rm x}}\left({V_D}^{\rm ON}+V_{out}\right)=0 \tag{8}$$

$$\frac{d{I_{L_{\rm r}}}^{(1)}(\omega t)}{d\omega t}=\frac{1}{\omega(L_{\rm r}+L_{\rm x})}\left(-\omega^2 C_{\rm i}L_{\rm x}\frac{d^2 {V_{C_{\rm i}}}^{(1)}(\omega t)}{d(\omega t)^2}+{V_D}^{\rm ON}+V_{out}\right) \tag{9}$$

The generic solution for (8) is

$${V_{C_{\rm i}}}^{(1)}(\omega t)=c_{11}\cos\left(\beta_1\,\omega t\right)+c_{12}\sin\left(\beta_1\,\omega t\right)+k_{11} \tag{10}$$

where $\beta_1=\sqrt{\frac{L_{\rm r}+L_{\rm x}}{\omega^2 C_{\rm i}(L_{\rm i}L_{\rm x}+L_{\rm r}L_{\rm x}+L_{\rm i}L_{\rm r})}}$ is obtained by solving the associated homogeneous characteristic equation, $k_{11}=\frac{(L_{\rm r}+L_{\rm x})V_{in}-L_{\rm x}\left({V_D}^{\rm ON}+V_{out}\right)}{L_{\rm r}+L_{\rm x}}$ and c_{11}, c_{12} are coefficients that depend on the initial conditions (7). At this point, a solution for (9) can be easily obtained as

$${I_{L_{\rm r}}}^{(1)}(\omega t)=I_{L_{\rm r}}^0+k_{12}\beta_1\left(c_{11}\sin\left(\beta_1\omega t\right)-c_{12}\cos\left(\beta_1\omega t\right)\right)+k_{13}\omega t \tag{11}$$

where $k_{12}=\frac{\omega C_{\rm i}L_{\rm x}}{L_{\rm r}+L_{\rm x}}$, and $k_{13}=\frac{{V_D}^{\rm ON}+V_{out}}{\omega(L_{\rm r}+L_{\rm x})}$.

At $\omega t=\theta_2$ the rectifier current falls down to zero, the diode turns-off and Z_2 starts. The value of θ_2 can be (numerically) computed from (11) by solving ${I_{L_{\rm r}}}^{(1)}(\theta_2)=0$ under the constraint $0<\theta_2<\theta_3$, while the evolution of the zone is regulated by (1), (3) and (5), constituting the fourth order system of differential equations

$$\begin{cases} \omega^2 C_{\rm i}\left(L_{\rm i}+L_{\rm x}\right)\dfrac{d^2 {V_{C_{\rm i}}}^{(2)}(\omega t)}{d(\omega t)^2}+\omega^2 C_{\rm i}L_{\rm x}\dfrac{d^2 {V_{C_{\rm r}}}^{(2)}(\omega t)}{d(\omega t)^2}+{V_{C_{\rm i}}}^{(2)}(\omega t)-V_{in}=0 \\ \omega^2 C_{\rm i}L_{\rm x}\dfrac{d^2 {V_{C_{\rm i}}}^{(2)}(\omega t)}{d(\omega t)^2}+\omega^2 C_{\rm r}(L_{\rm r}+L_{\rm x})\dfrac{d^2 {V_{C_{\rm r}}}^{(2)}(\omega t)}{d(\omega t)^2}+{V_{C_{\rm r}}}^{(2)}(\omega t)-V_{out}=0 \end{cases} \tag{12}$$

subject to the initial conditions

$$\begin{cases} {V_{C_{\rm i}}}^{(2)}(\theta_2)={V_{C_{\rm i}}}^{(1)}(\theta_2) \\ {V_{C_{\rm r}}}^{(2)}(\theta_2)=-{V_D}^{\rm ON} \\ \left.\dfrac{d{V_{C_{\rm i}}}^{(2)}(\omega t)}{d\omega t}\right|_{\omega t=\theta_2}=\dfrac{{I_{L_{\rm i}}}^{(2)}(\theta_2)}{\omega C_{\rm i}}=\dfrac{{I_{L_{\rm i}}}^{(1)}(\theta_2)}{\omega C_{\rm i}} \\ \left.\dfrac{d{V_{C_{\rm r}}}^{(2)}(\omega t)}{d\omega t}\right|_{\omega t=\theta_2}=\dfrac{{I_{L_{\rm r}}}^{(2)}(\theta_2)}{\omega C_{\rm r}}=\dfrac{{I_{L_{\rm r}}}^{(1)}(\theta_2)}{\omega C_{\rm r}} \end{cases} \tag{13}$$

By defining $\mathbf{V}^{(2)}(\omega t)=\{{V_{C_{\rm i}}}^{(2)}(\omega t),{V_{C_{\rm r}}}^{(2)}(\omega t)\}^{\intercal}$, and considering the equivalent matrix form for (12)

$$\mathbf{M}\,\frac{d^2\mathbf{V}^{(2)}(\omega t)}{d(\omega t)^2}=\mathbf{K}\cdot\mathbf{V}^{(2)}(\omega t)+\mathbf{k}_2$$

with $\mathbf{M},\mathbf{K}\in\mathbb{R}^{2\times 2}$, and $\mathbf{k}_2\in\mathbb{R}^2$, one can write the system solution as

$$\mathbf{V}^{(2)}(\omega t)=\sum_{j=1}^{2}\left(a_j\cos\left(\beta_{2,j}(\omega t-\theta_2)\right)+\frac{b_j}{\beta_{2,j}}\sin\left(\beta_{2,j}(\omega t-\theta_2)\right)\right)\mathbf{w}_j+\mathbf{k}_2$$

with $\beta_{2,j}=\sqrt{-\lambda_j}$, $j=1,2$, $\{\lambda_j,\mathbf{w}_j\}$ representing the eigenpairs of the matrix $\mathbf{M}^{-1}\cdot\mathbf{K}$, and a_j, b_j coefficients depending on the initial conditions (13).

The zone Z_3 begins at $\omega t=\theta_3$, when the MOS switch is externally turned-on. The evolution is regulated by the third order system given by (1), (2) and (5):

$$\begin{cases} \omega(L_{\rm i}+L_{\rm x})\dfrac{d{I_{L_{\rm i}}}^{(3)}(\omega t)}{d\omega t}+\omega^2 C_{\rm r}L_{\rm x}\dfrac{d^2 {V_{C_{\rm r}}}^{(3)}(\omega t)}{d(\omega t)^2}-V_{in}=0 \\ \omega L_{\rm x}\dfrac{d{I_{L_{\rm i}}}^{(3)}(\omega t)}{d\omega t}+\omega^2 C_{\rm r}\left(L_{\rm r}+L_{\rm x}\right)\dfrac{d^2 {V_{C_{\rm r}}}^{(3)}(\omega t)}{d(\omega t)^2}+{V_{C_{\rm r}}}^{(3)}(\omega t)-V_{out}=0 \end{cases}$$

subject to the initial conditions

$$\begin{cases} {V_{C_{\rm r}}}^{(3)}(\theta_3)={V_{C_{\rm r}}}^{(2)}(\theta_3) \\ \left.\dfrac{d{V_{C_{\rm r}}}^{(3)}(\omega t)}{d\omega t}\right|_{\omega t=\theta_3}=\dfrac{{I_{L_{\rm r}}}^{(3)}(\theta_3)}{\omega C_{\rm r}}=\dfrac{{I_{L_{\rm r}}}^{(2)}(\theta_3)}{\omega C_{\rm r}} \\ {I_{L_{\rm i}}}^{(3)}(\theta_3)={I_{L_{\rm i}}}^{(2)}(\theta_3) \end{cases} \tag{14}$$

The solutions can be easily achieved from (10) and (11) due to the circuit symmetry

$$\begin{cases} {V_{C_{\rm r}}}^{(3)}(\omega t)=c_{31}\cos\left(\beta_3(\omega t-\theta_3)\right)+c_{32}\sin\left(\beta_3(\omega t-\theta_3)\right)+k_{31} \\ {I_{L_{\rm i}}}^{(3)}(\omega t)=I_{L_{\rm i}}(\theta_3)+k_{32}\beta_3\left(c_{31}\sin\left(\beta_3(\omega t-\theta_3)\right)-c_{32}\cos\left(\beta_3(\omega t-\theta_3)\right)\right)+k_{33}\omega t \end{cases}$$

with $\beta_3=\sqrt{\frac{L_{\rm i}+L_{\rm x}}{\omega^2 C_{\rm r}(L_{\rm i}L_{\rm x}+L_{\rm r}L_{\rm x}+L_{\rm i}L_{\rm r})}}$, $k_{31}=\frac{(L_{\rm i}+L_{\rm x})V_{out}-L_{\rm x}V_{in}}{L_{\rm i}+L{\rm x}}$, $k_{32}=\frac{\omega C_{\rm r}L_{\rm x}}{L_{\rm i}+L_{\rm x}}$, $k_{33}=\frac{V_{in}}{\omega(L_{\rm i}+L_{\rm x})}$, and c_{31}, c_{32} depending on the initial conditions (14).

Finally, Z_4, where both switching devices are ON, begins at $\omega t=\theta_4$ when the forward voltage of the diode reaches the threshold ${V_D}^{\rm ON}$. The value of θ_4 can be computed by solving ${V_{C_{\rm r}}}^{(3)}(\theta_4)=-{V_{\rm D}}^{\rm ON}$, with $\theta_3<\theta_4<2\pi$. The circuit evolution is given by (1), (2) and (4), that can be reduced to the second order system

$$\begin{cases} \omega\left(L_{\rm i}+L_{\rm x}\right)\dfrac{d{I_{L_{\rm i}}}^{(4)}(\omega t)}{d\omega t}+\omega L_{\rm x}\dfrac{d{I_{L_{\rm r}}}^{(4)}(\omega t)}{d\omega t}-V_{in}=0 \\ \omega L_{\rm x}\dfrac{d{I_{L_{\rm i}}}^{(4)}(\omega t)}{d\omega t}+\omega\left(L_{\rm r}+L_{\rm x}\right)\dfrac{d{I_{L_{\rm r}}}^{(4)}(\omega t)}{d\omega t}-{V_D}^{\rm ON}-V_{out}=0 \end{cases}$$

subject to the initial conditions

$$\begin{cases} {I_{L_{\rm i}}}^{(4)}(\theta_4)={I_{L_{\rm i}}}^{(3)}(\theta_4) \\ {I_{L_{\rm r}}}^{(4)}(\theta_4)={I_{L_{\rm r}}}^{(3)}(\theta_4) \end{cases}$$

The solution is made of two straight line waveforms

$$\begin{cases} {I_{L_{\rm i}}}^{(4)}(\omega t)={I_{L_{\rm i}}}^{(4)}(\theta_4)+k_{41}(\omega t-\theta_4) \\ {I_{L_{\rm r}}}^{(4)}(\omega t)={I_{L_{\rm r}}}^{(4)}(\theta_4)+k_{42}(\omega t-\theta_4) \end{cases}$$

This is the author's version of the article that has been presented at IEEE ISCAS2015
The editorial version of the paper is available at http://dx.doi.org/10.1109/ISCAS.2015.7169189

with angular coefficients $k_{41} = \frac{V_{in}}{\omega(L_\mathrm{i}+L_\mathrm{x})} - \frac{L_\mathrm{x}}{\omega(L_\mathrm{i}L_\mathrm{x}+L_\mathrm{r}L_\mathrm{x}+L_\mathrm{i}L_\mathrm{r})}\left(V_D^{\mathrm{ON}} + V_{out} - \frac{L_\mathrm{x}}{L_\mathrm{i}+L_\mathrm{x}}V_{in}\right)$, $k_{42} = \frac{L_\mathrm{i}+L_\mathrm{x}}{\omega(L_\mathrm{i}L_\mathrm{x}+L_\mathrm{r}L_\mathrm{x}+L_\mathrm{i}L_\mathrm{r})}\left(V_D^{\mathrm{ON}} + V_{out} - \frac{L_\mathrm{x}}{L_\mathrm{i}+L_\mathrm{x}}V_{in}\right)$. The zone Z_4 ends at $\omega t = 2\pi$ when the MOS switch is turned-off and the described behavior is repeated periodically.

The above procedure allows us to get *exact* expressions for all voltage and current signals of the converter. Interestingly, the achieved expressions depend only on twelve parameters, i.e., the *initial conditions* $\mathbf{ic} = \left\{I_{L_\mathrm{i}}^0, I_{L_\mathrm{r}}^0\right\}$, the *converter specifications* $\mathbf{r} = \left\{V_{in}, V_{out}, V_D{}^{\mathrm{ON}}, \omega, \theta_3\right\}$ and the values of the *reactive elements* $\mathbf{x} = \{C_\mathrm{i}, C_\mathrm{r}, L_\mathrm{i}, L_\mathrm{x}, L_\mathrm{r}\}$.

IV. Design Methodology

The target of the design procedure is to find the complete set of *design parameters* that, once *steady state* is achieved, satisfies the ZVS, ZCS and output power operating conditions. Thanks to the piecewise mathematical model provided in the last section we can formalize the aforementioned operating constraints with the following system of non-linear equations

$$\begin{cases} I_{L_\mathrm{i}}^{(4)}(2\pi) - I_{L_\mathrm{i}}^0 = 0 & \text{(15a)} \\ I_{L_\mathrm{r}}^{(4)}(2\pi) - I_{L_\mathrm{r}}^0 = 0 & \text{(15b)} \\ V_{C_\mathrm{i}}^{(2)}(\theta_3) = 0 & \text{(15c)} \\ I_{L_\mathrm{i}}^{(2)}(\theta_3) = 0 & \text{(15d)} \\ P_{out} + \frac{V_{out}}{2\pi}\left(\int_0^{\theta_2} I_{L_\mathrm{r}}^{(1)}(\omega t)\,d\omega t + \int_{\theta_4}^{2\pi} I_{L_\mathrm{r}}^{(4)}(\omega t)\,d\omega t\right) = 0 & \text{(15e)} \end{cases}$$

Equations (15a) and (15b) ensure *steady state operation*, achieved when the values of the current signals at $\omega t = 2\pi$ match **ic** (note that a similar condition for the voltage signals is implicitly satisfied). *Optimum class-E operation* is accomplished assuring (15c) and (15d) at the end of Z_2, that represent respectively ZVS and ZCS. Lastly, (15e) is the constraint on the output power at full load, that can be computed by integrating the output current $-I_{L_\mathrm{r}}(\omega t)$ over a period. Note that, since in Z_2 and Z_3 this current is flowing through the capacitor C_r, that is assumed ideal, we do not have any contribution to the output power in these zones, and only Z_1 and Z_4, when the current is flowing through the diode, have to be considered.

To exemplify our procedure, let us consider the design of a 5 W output power converter based on the schematic of Fig. 1(a) with $f_s = 30\,\mathrm{MHz}$ and featuring a 1:1 coupling transformer. Let us assume that **r** is completely specified with $V_{in} = 3.3V$, $V_{out} = 5V$, $V_D{}^{\mathrm{ON}} = 0.7V$, $\omega = 2\pi f_s = 188.5 \times 10^6\,\mathrm{rad/s}$, $\theta_3 = \pi\,\mathrm{rad}$ (i.e. 50% duty cycle). There are seven design parameters to be determined, given by **ic** and **x**, and only five constraints according to (15). This means that, among **ic** and **x**, five parameters are *constrained* while two are actually *free design parameters* to be set by the designer. In our example, the value of L_i is linked, as explained in Section II, to the value of L_x by means of the coupling coefficient k, that is assumed $k = 0.95$. The last degree of freedom is exploited setting $L_\mathrm{r} = L_\mathrm{x}$. With the above defined specifications, we are able to solve (15) with *Wolfram Mathematica* software, leading to $C_\mathrm{i} = 1.61\,\mathrm{nF}$, $C_\mathrm{r} = 899\,\mathrm{pF}$, $L_\mathrm{x} = 19.25\,\mathrm{nH}$, $I_{L_\mathrm{i}}^0 = 4.44\,\mathrm{A}$, $I_{L_\mathrm{r}}^0 = -2.14\,\mathrm{A}$ and the diode turn-off and turn-on instants $\theta_2 = 0.98\,\mathrm{rad}$, $\theta_4 = 4.45\,\mathrm{rad}$. The resulting voltage and current waveforms, according to the developed mathematical model, are depicted in Fig. 3. As clearly observable, both the steady state and ZVS/ZCS conditions are perfectly achieved.

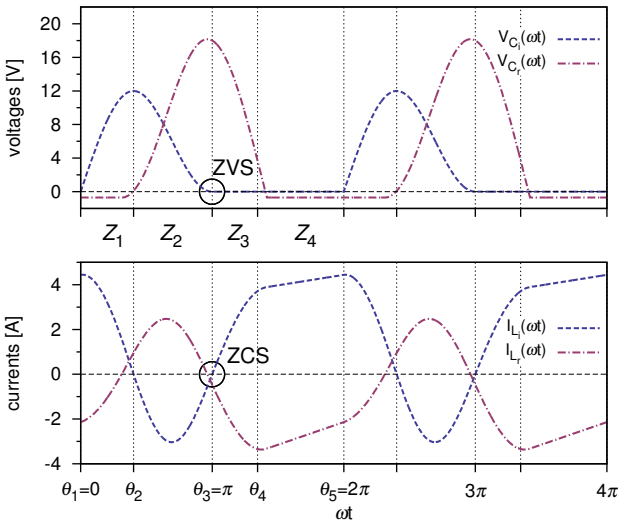

Fig. 3. Class-E converter waveforms obtained following the proposed analysis and design methodology.

V. Conclusion

This paper presents an accurate design methodology based on a differential-equation analysis for a class-E resonant dc-dc power converter topology. The small number of passive elements allows to develop a semi-analytical design procedure, that, unlike previous design methods, is not based on any kind of approximation and permits to get the whole circuit design without requiring time-extensive parametric sweeps across circuit parameters. A design example is provided to show both the simpleness and the effectiveness of the proposed approach.

References

[1] J. Rivas, D. Jackson, O. Leitermann, A. Sagneri, Y. Han, and D. Perreault, "Design Considerations for Very High Frequency dc-dc Converters," in *2006 IEEE Power Electronics Specialists Conference*, Jun. 2006, pp. 1–11.

[2] R. Gutmann, "Application of RF Circuit Design Principles to Distributed Power Converters," *IEEE Trans. Ind. Electron. and Control Instr.*, vol. IECI-27, no. 3, pp. 156–164, Aug. 1980.

[3] R. Redl, B. Molnar, and N. Sokal, "Class E Resonant Regulated DC/DC Power Converters: Analysis of Operations, and Experimental Results at 1.5 MHz," *IEEE Trans. Power Electron.*, vol. PE-1, no. 2, pp. 111–120, Apr. 1986.

[4] R. Pilawa-Podgurski, A. Sagneri, J. Rivas, D. Anderson, and D. Perreault, "Very-high-frequency resonant boost converters," *IEEE Trans. Power Electron.*, vol. 24, no. 6, pp. 1654–1665, Jun. 2009.

[5] M. Kazimierczuk and J. Jozwik, "Resonant DC/DC converter with class-E inverter and class-E rectifier," *IEEE Trans. Ind. Electron.*, vol. 36, no. 4, pp. 468–478, Nov. 1989.

[6] N. Sokal and A. Sokal, "Class E-A new class of high-efficiency tuned single-ended switching power amplifiers," *IEEE J. Solid-State Circuits*, vol. 10, no. 3, pp. 168–176, Jun. 1975.

[7] A. Ivascu, M. Kazimierczuk, and S. Birca-Galateanu, "Class E resonant low dv/dt rectifier," *IEEE Trans. Circuits Syst. I, Fundam. Theory Appl.*, vol. 39, no. 8, pp. 604–613, Aug. 1992.

[8] J. M. Burkhart, R. Korsunsky, and D. J. Perreault, "Design Methodology for a Very High Frequency Resonant Boost Converter," *IEEE Trans. Power Electron.*, vol. 28, no. 4, pp. 1929–1937, Apr. 2013.